

# ***Gain-Momentum Locking in a Chiral-Gain Medium***

*João C. Serra<sup>1,\*</sup>, Nader Engheta<sup>2</sup>, Mário G. Silveirinha<sup>1,†</sup>*

*<sup>(1)</sup> University of Lisbon–Instituto Superior Técnico and Instituto de Telecomunicações, Avenida Rovisco Pais, 1, 1049-001 Lisboa, Portugal*

*<sup>(2)</sup> University of Pennsylvania, Department of Electrical and Systems Engineering, Philadelphia, PA 19104, U.S.A.*

## **Abstract**

Conventional optical materials are characterized by either a dissipative response, which results in polarization-independent absorption, or by a gain response that leads to wave amplification. In this study, we explore the potential of a peculiar class of materials with chiral-gain properties, where gain selectively amplifies waves of one polarization handedness, while dissipation suppresses the opposite handedness. We uncover a novel phenomenon, “gain-momentum locking”, at the boundary of these chiral-gain materials, where surface plasmons are uniquely amplified or attenuated based on their direction of propagation. This effect, driven by the interplay between spin-momentum locking and polarization-sensitive non-Hermitian responses, enables precise control over unidirectional wave propagation. Our findings open the door to photonic devices with unprecedented capabilities, such as lossless unidirectional edge-wave propagation and the generation of light with intrinsic orbital angular momentum.

---

\* E-mail: [joao.serra@lx.it.pt](mailto:joao.serra@lx.it.pt)

† To whom correspondence should be addressed: [mario.silveirinha@tecnico.ulisboa.pt](mailto:mario.silveirinha@tecnico.ulisboa.pt)

## Main Text

The propagation properties in a non-magnetic medium are tailored by the photonic dispersion and isofrequency surfaces, governed by the Hermitian part  $\bar{\epsilon}' = (\bar{\epsilon} + \bar{\epsilon}^\dagger) / 2$  of the permittivity tensor  $\bar{\epsilon}$ . When all eigenvalues of  $\bar{\epsilon}'$  are positive, the isofrequency contours assume an ellipsoidal shape, indicative of dielectric-type behavior. Conversely, if all eigenvalues are negative, the material behaves akin to a metal, not supporting wave propagation. More uniquely, when the tensor possesses both positive and negative eigenvalues, the medium displays a dual response characterized by direction-dependent band gaps. These are known as hyperbolic-type materials, such as hexagonal boron nitride. Within this category, type I and type II systems have one or two negative eigenvalues, respectively [1-3].

Evidently, the response of realistic materials is usually non-Hermitian. In such cases, the material response can be conveniently decomposed as  $\bar{\epsilon} = \bar{\epsilon}' + i\bar{\epsilon}''$ , where the Hermitian part of the response  $\bar{\epsilon}'$  is defined as before and the non-Hermitian part is given by  $\bar{\epsilon}'' = (\bar{\epsilon} - \bar{\epsilon}^\dagger) / (2i)$ . Both components ( $\bar{\epsilon}'$  and  $\bar{\epsilon}''$ ) are Hermitian tensors with real-valued eigenvalues. The non-Hermitian component  $\bar{\epsilon}''$  governs the power transfer between the medium and the wave. Specifically, in the time-harmonic regime, the average power per unit volume transferred from the wave to the material (dissipated power) is given by  $p_d = \frac{1}{2} \omega \epsilon_0 \mathbf{E}^* \cdot \bar{\epsilon}'' \cdot \mathbf{E}$  [4]. This formula holds true for dispersive and nonlocal systems. For a passive material, the eigenvalues must be positive to ensure  $p_d > 0$ . Conversely, in

standard gain materials (e.g., within a laser cavity), when gain overcomes dissipative effects,  $p_d < 0$  and all the eigenvalues are negative.

The focus of this article is to consider an intermediate scenario where  $\bar{\epsilon}''$  is indefinite, having eigenvalues of both signs. Under such conditions, the material can exhibit either gain or loss depending on the wave polarization. This possibility was recently explored in the context of a photonic analogue of semiconductor transistors [5]. Additionally, it has been demonstrated that indefinite-gain responses can be implemented in electrically biased low-symmetry materials with nontrivial Berry curvature dipoles [6, 7], as well as in other optically pumped platforms [8].

Here, we consider an electric response consistent with that of the idealized MOSFET-metamaterial studied in Ref. [5], with the relative permittivity tensor given by

$$\bar{\epsilon} = \begin{pmatrix} \epsilon_{xx} & 0 & \epsilon_{xz} \\ 0 & \epsilon_{yy} & 0 \\ 0 & 0 & \epsilon_{zz} \end{pmatrix}. \quad (1)$$

First, we assume that the permittivity tensor (1) is real-valued and frequency-independent. In such a case, the non-Hermitian component  $\bar{\epsilon}''$  is anti-symmetric and it can be written in terms of the vector  $\mathbf{\Omega} = +\frac{\epsilon_{xz}}{2}\hat{\mathbf{y}}$  as  $\bar{\epsilon}'' = -i\mathbf{\Omega} \times \mathbf{1}$ . We shall refer to  $\mathbf{\Omega}$  as the *gain vector*.

The nontrivial eigenvalues of  $\bar{\epsilon}''$  are  $\pm\frac{\epsilon_{xz}}{2}$  and the corresponding eigenvectors are the circular polarization states  $\mathbf{e}_{\pm} = \frac{1}{\sqrt{2}}(\hat{\mathbf{x}} \pm i\hat{\mathbf{z}})$ .

Interestingly, the non-Hermitian response has chiral properties as the power transfer is governed by the quadratic form  $p_d = \frac{-1}{2}\omega\epsilon_0|\mathbf{E}|^2\mathbf{\Omega} \cdot \boldsymbol{\sigma}$ , which depends on the relative

orientation of the spin angular momentum of light  $\boldsymbol{\sigma} = i(\mathbf{E} \times \mathbf{E}^*)/|\mathbf{E}|^2$  with respect to the gain vector  $\boldsymbol{\Omega}$  [9]. Remarkably, when the spin angular momentum is parallel (anti-parallel) to the gain vector, the medium supplies energy to (absorbs energy from) the wave. Therefore, when  $\varepsilon_{xz} > 0$ , the polarization state  $\mathbf{e}_+$  activates “dissipation”, whereas the orthogonal polarization state  $\mathbf{e}_-$  activates optical gain.

For simplicity, we restrict our attention to propagation in the  $xoz$  plane with the magnetic field oriented along the  $y$  direction (aligned with  $\boldsymbol{\Omega}$ ), so that  $\mathbf{H} = H_y(x, z)\hat{\mathbf{y}}$ . It is shown in the supplementary information that provided  $|\varepsilon_{xz}| \leq 2\sqrt{\varepsilon_{xx}\varepsilon_{zz}}$  the bulk material response is stable for propagation in the  $xoz$  plane [10]. In these conditions, the bulk modes are linearly polarized [10] and thereby are unaffected by gain or dissipation, as  $p_d$  vanishes for such a case.

Notably, surface plasmons (SPPs) – which naturally occur at dielectric-metal interfaces – possess inherent chiral properties. The “spin” of surface plasmons is linked to their direction of propagation, through a property known as “spin-momentum locking” [11, 12]. Therefore, intuitively one may expect that materials exhibiting chiral-gain can amplify plasmons whose chirality aligns with the gain vector, while suppressing those with opposite chirality (Fig. 1a).

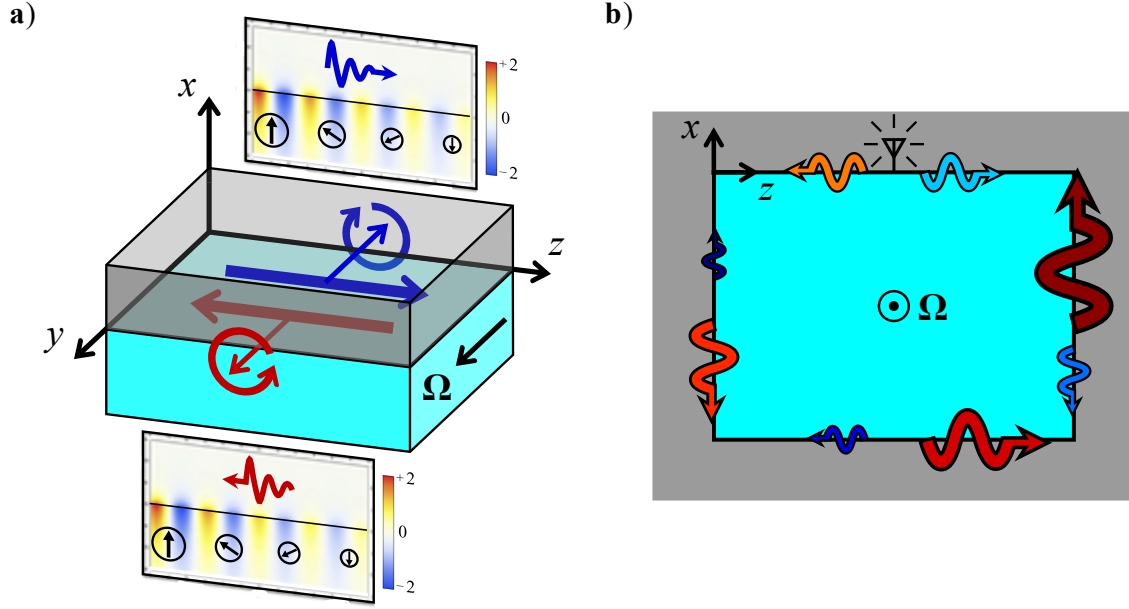


**Fig. 1 (a)** Interface between a chiral-gain medium (region  $x < 0$ , shaded in green) and an isotropic material (metal;  $x > 0$ , shaded in gray). Due to the spin-momentum locking, surface plasmons have an inherent chirality. The oriented blue and red circles represent the spin  $\sigma$  of the plasmons in the chiral-gain material side of the interface for waves propagating along  $+z$  and  $-z$ , respectively. The chiral-gain medium amplifies plasmons whose spin aligns with the gain vector  $\Omega$  (directed along  $+y$ ) and suppresses those with opposite spin. **(b)** Illustration of an “edge-cavity” laser based on a chiral-gain medium and a metallic coating. The wave that propagates in the counter-clockwise (clockwise) direction is amplified (attenuated). Hence, the orbital angular momentum of the lasing mode is locked to the direction of the gain vector  $\Omega$ . Lighter/darker colors represent the edge states at earlier/later time instants.

In order to demonstrate such “gain-momentum locking”, we consider the flat interface represented in Fig. 1a between a chiral-gain medium ( $x < 0$ ) described by the permittivity

tensor (1) and a metal ( $x > 0$ ) with relative permittivity  $\varepsilon_m(\omega) = 1 - \frac{\omega_m^2}{\omega(\omega + i\Gamma)}$ . Here,  $\omega_m$

is the metal plasma frequency and  $\Gamma$  is the collision frequency.

For simplicity, we start by analyzing the system in the quasi-static regime. This corresponds to the spectral region characterized by  $\omega^2 \ll c^2 \mathbf{k} \cdot \mathbf{k}$ , where the magnetic field is negligible ( $\mathbf{H} \approx \mathbf{0}$ ) and the electric field is determined by a scalar potential ( $\mathbf{E} \approx -\nabla \phi$ ). Since the system has continuous translational symmetry in the  $yoz$  plane, the electric potential associated with a surface plasmon is of the form:

$$\phi(x, z, t) = \phi_0 e^{-i\omega t} e^{iqz} \times \begin{cases} e^{+\gamma_{\text{CO}} x}, & x < 0 \\ e^{-\gamma_{\text{m0}} x}, & x > 0 \end{cases}, \quad (2)$$

where  $q$  is the propagation constant along  $z$ . The electric potential must satisfy Gauss's law  $\nabla \cdot (\bar{\boldsymbol{\varepsilon}} \cdot \nabla \phi) = 0$ , which for plane waves (spatial variation  $e^{i\mathbf{k} \cdot \mathbf{r}}$ ) reduces to  $\mathbf{k} \cdot \bar{\boldsymbol{\varepsilon}} \cdot \mathbf{k} = 0$ .

From here, it is found that the attenuation constants along  $z$  are  $\gamma_{\text{m0}} = \sqrt{q^2}$  in the metal

region, and  $\gamma_{\text{CO}} = \sqrt{q^2 \left( \frac{\varepsilon_{zz}}{\varepsilon_{xx}} - \frac{\varepsilon_{xz}^2}{4\varepsilon_{xx}^2} \right) - iq \frac{\varepsilon_{xz}}{2\varepsilon_{xx}}}$  in the chiral-gain region.

Let us suppose that the chiral-gain response is a weak perturbation of the response of an isotropic dielectric ( $\varepsilon_{xx} \approx \varepsilon_{zz} \gg |\varepsilon_{xz}|$ ), so that  $\gamma_{\text{CO}} \approx \gamma_{\text{m0}} = \sqrt{q^2}$ . Then, the electric field in the chiral-gain region is roughly  $\mathbf{E} \approx -|q| \phi_0 e^{-i\omega t} e^{iqz} e^{+|q|x} [\hat{\mathbf{x}} + i \text{sgn}(q) \hat{\mathbf{z}}]$ , for  $q$  real-valued. As expected, the orientation of the transverse spin of the plasmons,  $\boldsymbol{\sigma} = -\text{sgn}(q) \hat{\mathbf{y}}$  depends on the direction of propagation [11-12]. If the gain vector  $\boldsymbol{\Omega} = +\frac{\varepsilon_{xz}}{2} \hat{\mathbf{y}}$  points along  $+y$ , the transverse spin  $\boldsymbol{\sigma}$  is parallel (anti-parallel) to  $\boldsymbol{\Omega}$  for propagation along  $-z$  ( $+z$ ). Consequently, these directions of propagation correspond to conditions of plasmon amplification and attenuation, respectively, as illustrated in Fig. 1a.

To confirm this result, next we derive the quasi-static dispersion of the surface plasmons. To this end, we enforce the continuity of the normal component of the electric displacement vector at the interface ( $\hat{\mathbf{x}} \cdot \mathbf{D}|_{x=0^-} = \hat{\mathbf{x}} \cdot \mathbf{D}|_{x=0^+}$  with  $\mathbf{D} = -\varepsilon_0 \bar{\varepsilon} \cdot \nabla \phi$ ). This yields:

$$\gamma_{m0} \varepsilon_m(\omega) + \gamma_{c0} \varepsilon_{xx} + iq \varepsilon_{xz} = 0. \quad (3)$$

The attenuation coefficients must reside in the complex right half-plane, i.e.,  $\text{Re}\{\gamma_{m0/c0}\} > 0$  to confine the energy at the interface  $x = 0$ .

Let us first analyze excitations with  $q$  real-valued and  $\omega = \omega' + i\omega''$ . These correspond to the natural modes of a ring-type edge-resonator in the  $x = 0$  plane (see [13] for a related discussion). For passive resonators, it is necessary that  $\omega'' < 0$ , indicating that the excitation relaxes over time ( $e^{-i\omega t} = e^{-i\omega' t} e^{\omega'' t}$ ); conversely,  $\omega'' > 0$  is indicative of a lasing mode. Solving Eq. (3) with respect to the oscillation frequency, it is found that in  $\Gamma = 0^+$  limit:

$$\omega|_{\text{QS}} = \frac{\omega_m}{\left(1 + \sqrt{\varepsilon_{xx} \varepsilon_{zz} - \frac{\varepsilon_{xz}^2}{4}} + i \text{sgn}(q) \frac{\varepsilon_{xz}}{2}\right)^{1/2}}. \quad (4)$$

When the chiral-gain response is nearly isotropic ( $\varepsilon_{xx} \approx \varepsilon_{zz} \gg |\varepsilon_{xz}|$ ), it follows that

$$\omega|_{\text{QS}} = \omega' + i\omega'' \approx \frac{\omega_m}{\sqrt{1 + \varepsilon_{xx}}} \left(1 - i \text{sgn}(q) \frac{\varepsilon_{xz}}{4(1 + \varepsilon_{xx})}\right). \text{ Thus, the gain rate } \omega'' \text{ of the surface}$$

plasmon excitations is locked to the direction of propagation. Specifically, in accordance with the relative orientation between  $\boldsymbol{\sigma}$  and  $\boldsymbol{\Omega}$ , it is observed that when  $\varepsilon_{xz} > 0$ , plasmons propagating along  $+z$  are attenuated ( $\omega'' < 0$ ), whereas those propagating along  $-z$  are amplified ( $\omega'' > 0$ ). Remarkably, even though each material individually exhibits a stable

bulk response, their combination generates an edge excitation that grows exponentially over time, corresponding to a lasing mode.

Figure 2a displays the exact complex frequency spectrum (blue lines) calculated by solving the full Maxwell's equations and incorporating retardation effects [10, Eq. (S6)]. The black lines represent the quasi-static solution discussed before, which, as expected, accurately describes the asymptotic behavior of the plasmons for large wave numbers. Consistent with the quasi-static analysis, the sign of the gain rate  $\omega''$  computed with the exact theory is locked to the sign of the propagation constant  $q$ . The results shown in Fig. 2a use a large gain parameter ( $\varepsilon_{xz} = 0.8$ ) to highlight the impact of the chiral-gain.

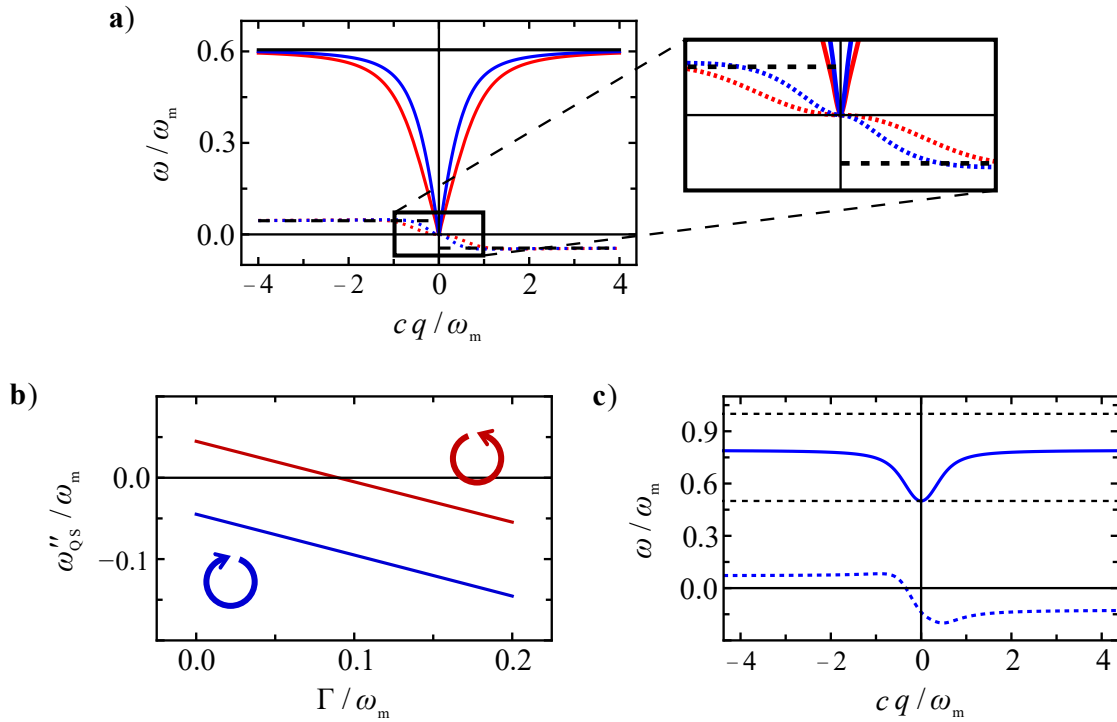


**Fig. 2** (a) Exact dispersion of the surface plasmons supported at an interface between a chiral-gain medium and a lossless Drude-type metal ( $\Gamma = 0$ ) at the  $x = 0$  (blue) and  $z = 0$  (red) interfaces. The black horizontal line represents the quasi-static solution. The figure shows the real (solid) and imaginary (dashed) parts of the frequency  $\omega' + i\omega''$  as a function of the wave number  $q \in \mathbb{R}$  for  $\varepsilon_{xx} = 1$ ,  $\varepsilon_{zz} = 3$ ,  $\varepsilon_{xz} = 0.8$ . (b) Growth rate



$\omega_{\text{QS}}''$  for highly-confined plasmons propagating in the CCW direction with  $\sigma \sim +\Omega$  (red) and in the CW direction with  $\sigma \sim -\Omega$  (blue) as a function of the Drude metal loss parameter  $\Gamma$ . The chiral-gain material has the same parameters as in (a). (c) Exact dispersion for plasmons propagating at the  $x=0$  interface between a (lossy) dispersive chiral-gain material and a lossless Drude metal. Real part: solid blue line; Imaginary part (multiplied by 100): dashed blue line. The horizontal dashed black lines represent the frequencies where  $\text{Re}[\varepsilon_{\text{c}}(\omega)]=0$  and  $\text{Re}[\varepsilon_{\text{m}}(\omega)]=0$ .

An interesting configuration for implementing an oscillator driven by the chiral-gain is illustrated in Fig. 1b. It consists of an edge-type resonator with four interfaces: two interfaces perpendicular to the  $x$  axis and another two perpendicular to the  $z$  axis. The propagation along the (horizontal) interfaces perpendicular to the  $x$  axis has been analyzed previously. Next, we investigate the propagation along the (vertical) interfaces perpendicular to the  $z$  direction, focusing on the left-hand side interface ( $z=0$ ). The quasi-static solution is constructed using the same steps as before. The electric potential in the chiral-gain medium ( $z>0$ ) is  $\phi(x, z, t) = \phi_0 e^{-i\omega t} e^{iqx} e^{-\tilde{\gamma}_{\text{c0}}z}$ , and in the metal region ( $z<0$ )  $\phi(x, z, t) = \phi_0 e^{-i\omega t} e^{iqx} e^{+\gamma_{\text{m0}}z}$ . Here,  $q$  represents the propagation constant of the plasmons and  $\gamma_{\text{m0}}$  is defined as before. The attenuation constant in the chiral-gain medium,

$$\tilde{\gamma}_{\text{c0}} = \sqrt{q^2 \left( \frac{\varepsilon_{xx}}{\varepsilon_{zz}} - \frac{\varepsilon_{xz}^2}{4\varepsilon_{zz}^2} \right) + iq \frac{\varepsilon_{xz}}{2\varepsilon_{zz}}},$$

is found by imposing  $\nabla \cdot (\bar{\varepsilon} \cdot \nabla \phi) = 0$  and the quasi-static

dispersion of the plasmons  $\gamma_{\text{m0}}\varepsilon_{\text{m}}(\omega) + \tilde{\gamma}_{\text{c0}}\varepsilon_{\text{zz}} = 0$  follows from the continuity of the normal component of the electric displacement vector. Solving this equation with respect to the oscillation frequency for a real-valued  $q$  in the  $\Gamma = 0^+$  limit, one finds precisely the same result as in Eq. (4). For both interfaces  $x=0$  and  $z=0$ ,  $q$  can be interpreted as the

propagation constant of the edge guide, with positive values indicating clockwise propagation. Thus, the propagation along the lateral interfaces is also governed by the gain-momentum locking discussed previously. As depicted in Fig. 1b, a field source near the top interface may excite surface plasmons propagating in both clockwise (CW) and counterclockwise (CCW) directions with respect to the gain vector  $\mathbf{\Omega}$  (oriented along the +y axis): while the former waves suffer attenuation, the latter are continuously amplified. Over time, the edge-resonator behaves as a unidirectional guide, because the CW modes are effectively suppressed. In practice, nonlinear effects will curb the exponential growth, resulting in a stable oscillator. Remarkably, the orbital angular momentum of the lasing modes of the edge-cavity is aligned with the direction of the gain vector  $\mathbf{\Omega}$ . We show in Fig. 2b that the amplification is suppressed for sufficiently high losses in the metal region.

A promising route to engineer a chiral-gain medium relies on low-symmetry materials with a Berry curvature dipole [6, 7], which have metal-type responses. To analyse how such a property affects the surface plasmons, next we consider a chiral-gain medium with a Drude-type dispersion. Specifically, we take  $\varepsilon_{xx} = \varepsilon_{zz} = \varepsilon_C(\omega)$  with

$$\varepsilon_C(\omega) = \varepsilon_\infty - \frac{\omega_p^2}{\omega(\omega + i\gamma)}. \text{ For simplicity, the gain parameter } \varepsilon_{xz} \text{ is assumed independent of}$$

frequency. In the supplementary information it is shown that the bulk response is stable for

$$\text{propagation in the } xoz \text{ plane provided } |\Sigma| < 1 - \frac{1}{(1 + \tilde{\gamma})^2} \text{ with } \Sigma = \frac{\varepsilon_{xz}}{\varepsilon_\infty} \text{ and } \tilde{\gamma} \equiv \sqrt{\varepsilon_\infty} \gamma / \omega_p.$$

We consider an interface between this dispersive chiral-gain medium and a metal with the same dispersive model as before. Evidently, such system can support plasmons in the range

where  $\text{Re}[\varepsilon_m(\omega)] < 0$  and  $\text{Re}[\varepsilon_c(\omega)] > 0$ , which corresponds to  $\omega_p / \sqrt{\varepsilon_\infty} < \omega < \omega_m$  in the  $\Gamma = \gamma = 0^+$  limit. Figure 2c represents the plasmons dispersion for a dispersive chiral-gain medium with  $\omega_p = 0.5\omega_m$ ,  $\varepsilon_\infty = 1$ ,  $\gamma = 0.00275\omega_m$ , and  $\varepsilon_{xz} = 0.01$ . As seen, the results are qualitatively similar to those in Fig. 2a, and for sufficiently large  $q$  the gain rate sign is strictly determined by the sign of the propagation constant. It is worth mentioning that the system also supports surface plasmons in the frequency range  $\omega_m < \omega < \omega_p / \sqrt{\varepsilon_\infty}$ , where  $\text{Re}[\varepsilon_m(\omega)] > 0$  and  $\text{Re}[\varepsilon_c(\omega)] < 0$ , however this configuration does not provide amplification of the edge-modes for a stable chiral-gain response.

Until now, our discussion has primarily focused on the natural modes of closed systems, such as resonators, where the boundary forms a closed loop. However, materials with chiral-gain can also be used to implement open systems. For instance, these materials can be utilized to develop unidirectional traveling wave amplifiers that operate on surface plasmons. To investigate these applications, next we consider plasmons characterized by a real-valued frequency  $\omega$ , driven by some external time-harmonic excitation. In such a context, the wave number of the plasmons becomes complex-valued:  $q = q' + iq''$ . We consider the same setup as in Fig. 1a, so that the propagation direction is along  $z$ , with a propagation factor  $e^{iqz} = e^{iq'z} e^{-q''z}$ . For simplicity, the chiral-gain medium is supposed dispersionless and the metal region lossless. We present in Fig. 3b the exact dispersion [10, Eq. (S6)] for edge states propagating along the  $z$  direction. Without chiral-gain ( $\varepsilon_{xz} = 0$ ), there is a spectral region with  $\varepsilon_m(\omega) < 0$  (shaded in gray) where surface plasmons cannot

propagate. Interestingly, in the presence of the chiral-gain response – no matter how small the gain parameter  $\varepsilon_{xz}$  is – there is no longer a stopband for  $\omega < \omega_m$ .

Figure 3c shows the projected dispersion in the complex  $q$  plane for different chiral-gain values  $\varepsilon_{xz}$ . The curves are coloured so that lighter (darker) tones correspond to lower (higher) frequencies. These results show that both plasmons propagating along the  $+z$  ( $q' > 0$ ) and  $-z$  ( $q' < 0$ ) directions are characterized by a positive  $q''$ . This implies that waves propagating along the  $+z$  ( $-z$ ) direction are attenuated (amplified), consistent with the results obtained for the closed resonator. Thus, the combination of the intrinsic spin-momentum locking of surface plasmons with the polarization-dependent non-Hermitian response of the chiral-gain material enables this system to act as a travelling wave amplifier/absorber depending on the direction of propagation of the edge modes.

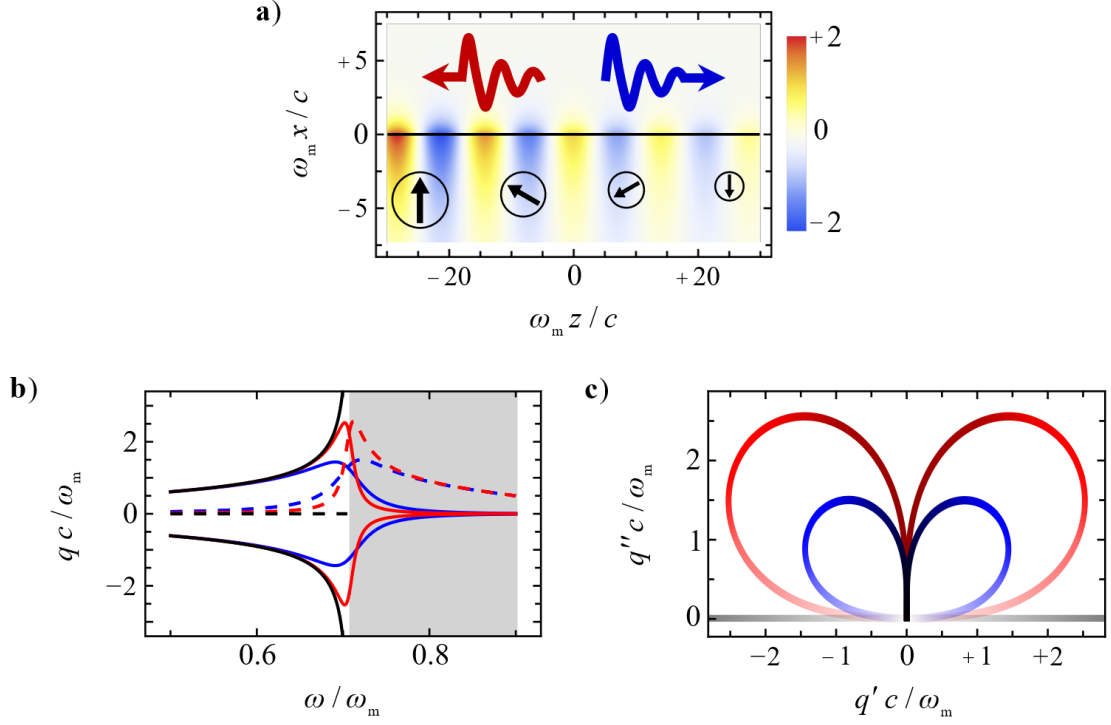


**Fig. 3** (a) Snapshot in time ( $t = 0$ ) of the magnetic field ( $H_y$ ) associated with a surface plasmon propagating at the interface  $x = 0$  between a dispersionless chiral-gain medium with  $\varepsilon_{xx} = \varepsilon_{zz} = 1$ ,  $\varepsilon_{xz} = 0.3$  ( $x < 0$ ) and a lossless Drude metal ( $x > 0$ ) for  $\omega = 0.4\omega_m$ . The arrows provide a qualitative representation of the instantaneous electric field distribution. (b) Exact dispersion of surface plasmons propagating with  $\omega \in \mathbb{R}$  at the interface represented in (a) for  $\varepsilon_{xz} = 0$  (black),  $\varepsilon_{xz} = 0.15$  (red) and  $\varepsilon_{xz} = 0.3$  (blue). We represent the real/imaginary component of the wave number  $q$  using full/dashed curves. The imaginary part of  $q$  is direction independent due to the time-reversal symmetry of the system. The gray area represents a stopband for surface plasmons in the absence of chiral-gain ( $\varepsilon_{xz} = 0$ ). (c) Projection of the exact dispersion of edge states in the complex wave number plane  $q = q' + iq''$  for different values of the chiral-gain parameter:  $\varepsilon_{xz} = 0$  (black),  $\varepsilon_{xz} = 0.15$  (red),  $\varepsilon_{xz} = 0.3$  (blue). Lighter/darker colors indicate smaller/larger frequencies in the range  $0 < \omega < \omega_m$ .

Figure 3a presents a snapshot of the magnetic field distribution associated with a surface plasmon at a specific oscillation frequency ( $\omega = 0.4\omega_m$ ). The arrows qualitatively indicate the orientation and strength of the electric field at the same instant. Interestingly, the dispersionless chiral-gain medium exhibits time-reversal symmetry because  $\bar{\epsilon}(\omega) = \bar{\epsilon}^*(\omega^*)$  [5, 8]. Therefore, in the case of a lossless Drude metal ( $\Gamma = 0^+$ ), our edge waveguide is also time-reversal symmetric. This implies that counter-propagating plasmons are connected through the time-reversal operation: if plasmons traveling along the  $+z$  direction are characterized by a certain field distribution  $(\mathbf{E}, \mathbf{H})$  and propagation constant  $q$ , then those traveling in the  $-z$  direction are described by the reverse field distribution  $(\mathbf{E}^*, -\mathbf{H}^*)$  with propagation constant  $-q^*$  [14-16]. Consequently, the time snapshots at  $t = 0$  for counter-propagating plasmons appear qualitatively similar, meaning that the density plot in Fig. 3a accurately represents plasmons moving in both the  $+z$  and  $-z$  directions. Furthermore,  $q'' = \text{Im}\{q\}$  is independent of the propagation direction. We note that the spatial variation ( $e^{+iqz}$ ) of the electric field in a time snapshot creates a perceived sense of rotation that is opposite to the actual time evolution of the electric field at a fixed point in space ( $e^{-i\omega t}$ ). Waves propagating along the  $+z$  direction exhibit left-elliptical polarization and experience attenuation, while those in the  $-z$  direction have right-elliptical polarization and undergo amplification, as depicted in Fig. 1b. Thus, chiral-gain media provide an interesting option for realizing unidirectional systems with gain. They potentially offer several advantages over time-modulated systems, which may require high modulation speeds [17-22], magnetically biased systems that need bulky biasing

circuits [23, 24], and systems employing drifting electrons, which demand large drift velocities [25-27].

To further validate our theory, we performed full-wave simulations using CST Microwave Studio [28]. Figure 4 depicts a time snapshot of the plasmons at the interface of a metal and a chiral-gain medium for a circularly shaped edge. As expected, when waves are excited to propagate in the clockwise direction (Fig. 4a), the plasmons are attenuated by the chiral-gain material. Conversely, when waves are excited to propagate in the counter-clockwise direction, the plasmons are amplified (Fig. 4b).

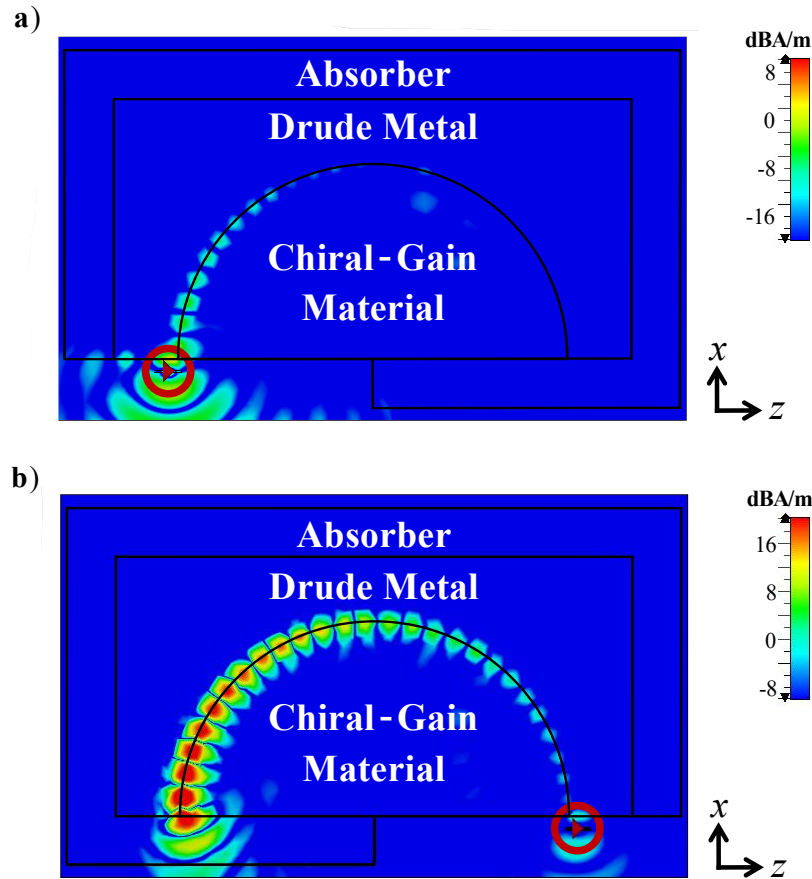


**Fig. 4** Full-wave simulations of the surface plasmons supported by the interface of a chiral-gain medium and a Drude metal. Excitation of (a) clockwise propagating plasmons and (b) counter-clockwise propagating

plasmons. The chiral-gain medium is characterized by  $\epsilon_{xx} = \epsilon_{zz} = 1$  and  $\epsilon_{xz} = 0.1$ . The metal is described by a Drude dispersion model with  $\omega_m = 2\pi \times 5.0$  GHz and  $\Gamma = 0^+$ . The density plots represent a time snapshot of the magnetic field at  $\omega = 2\pi \times 3.0$  GHz. The edge states are excited by half-wavelength dipoles located within the red circles.

In summary, we have characterized the propagation of edge states at the interface between a chiral-gain medium and a Drude metal using both quasi-static and exact formulations. We have shown that, despite the bulk response of the two materials being stable, the interface presents a gain-momentum locking effect. This intriguing outcome arises from the combination of the spin-momentum locking of surface plasmons and the polarization-dependent non-Hermitian response of the chiral-gain medium. We demonstrated how to leverage this property to design oscillators where the lasing modes have orbital angular momentum locked to the gain vector governing the chiral-gain, and to develop traveling wave amplifiers. Importantly, chiral-gain media can be used for loss-compensation of standard SPPs, enabling efficient propagation in photonic circuits. Additionally, the gain only needs to be applied within the confined footprint of the SPPs, making this approach practical and feasible for real-world applications. Given the combination of nonreciprocity and gain within a single material, chiral-gain media hold significant promise for advancing nanophotonic circuitry.

**Acknowledgements:** This work was partially funded by the Institution of Engineering and Technology (IET), by the Simons Foundation (Award 733700 for M.G.S. and Award 733684 to N.E.) and by Instituto de Telecomunicações under Project No. UIDB/50008/2020.

## References



- [1] D. R. Smith, D. Schurig, “Electromagnetic wave propagation in media with indefinite permittivity and permeability tensors”, *Phys. Rev. Lett.* **90**, 077405 (2003).
- [2] A. Poddubny, I. Iorsh, P. Belov, Y. Kivshar, “Hyperbolic metamaterials”, *Nat. Photon.*, **7**, (2013).
- [3] P. Shekhar, J. Atkinson, Z. Jacob, “Hyperbolic metamaterials: fundamentals and applications”, *Nano convergence* **1**, 1-17, (2014).
- [4] L. D. Landau, E. M. Lifshitz, *Electrodynamics of Continuous Media*, Course of theoretical Physics, vol.8, (Elsevier Butterworth-Heinemann, 2004).
- [5] S. Lannebère, D. E. Fernandes, T. A. Morgado, M. G. Silveirinha, “Nonreciprocal and Non-Hermitian Material Response Inspired by Semiconductor Transistors”, *Phys. Rev. Lett.* **128**, 013902 (2022).
- [6] T. G. Rappoport, T. A. Morgado, S. Lannebère, M. G. Silveirinha, “Engineering Transistorlike Optical Gain in Two-Dimensional Materials with Berry Curvature Dipoles”, *Phys. Rev. Lett.* **130**, 076901 (2023).
- [7] T. A. Morgado, T. G. Rappoport, S. S. Tsirkin, S. Lannebère, I. Souza, M. G. Silveirinha, “Non-Hermitian Linear Electrooptic Effect in 3D materials”, *Phys. Rev. B*, **109**, 245126, (2024).
- [8] S. Buddhiraju, A. Song, G. T. Papadakis, S. Fan, “Nonreciprocal Metamaterial Obeying Time-Reversal Symmetry”, *Phys. Rev. Lett.* **124**, 257403 (2020).
- [9] K. Y. Bliokh, A. Y. Bekshaev, F. Nori, “Extraordinary momentum and spin in evanescent waves”, *Nat. Comm.* **5**, 3300 (2014).
- [10] Supplementary online information with additional discussion on A) bulk stability of the non-dispersive material, B) dispersion of the edge states at an interface between a chiral-gain medium and an isotropic material, C) bulk stability of the dispersive material.
- [11] K. Y. Bliokh, D. Smirnova, F. Nori, “Quantum spin Hall effect of light”, *Science* **348**, 6242 (2015).
- [12] T. Van Mechelen, Z. Jacob, “Universal spin-momentum locking of evanescent waves”, *Optica* **3**, 118, (2016).
- [13] T. A. Morgado, M. G. Silveirinha, “Active graphene plasmonics with a drift-current bias”, *ACS Photonics*, **8**, 1129, 2021.
- [14] M. G. Silveirinha, “Time-reversal symmetry in Antenna Theory”, *Symmetry*, **11**, 486, (2019).
- [15] C. Caloz, A. Alù, S. Tretyakov, D. Sounas, K. Achouri, Z.-L. Deck-Léger, “Electromagnetic nonreciprocity”, *Phys. Rev. Applied* **10**, 047001 (2018).
- [16] V. S. Asadchy, M. S. Mirmoosa, A. Diaz-Rubio, S. Fan, S. A. Tretyakov, “Tutorial on electromagnetic nonreciprocity and its origins”, *Proc. IEEE* **108**, 1684 (2020).
- [17] Z. Yu, S. Fan, “Complete optical isolation created by indirect interband photonic transitions”, *Nat. Photonics* **3**, 91 (2009).
- [18] D. L. Sounas, C. Caloz, A. Alù, Giant non-reciprocity at the subwavelength scale using angular momentum-biased metamaterials, *Nat. Commun.* **4**, 2407 (2013).
- [19] T. T. Koutserimpas, R. Fleury, “Nonreciprocal gain in non-Hermitian time-Floquet systems”, *Phys. Rev. Lett.* **120**, 087401 (2018).

- [20] P. A. Huidobro, M. G. Silveirinha, E. Galiffi, J. B. Pendry, “Homogenization Theory of Space-Time Metamaterials”, *Phys. Rev. Applied* **16**, 014044 (2021).
- [21] E. Galiffi, R. Tirele, S. Yin, H. Li, S. Vezzoli, P. A. Huidobro, M. G. Silveirinha, R. Sapienza, A. Alù, J. B. Pendry, “Photonics of time-varying media”, *Adv. Photon.* **4** (1), 014002 (2022).
- [22] J. C. Serra, M. G. Silveirinha, “Rotating spacetime modulation: Topological phases and spacetime Haldane model”, *Phys. Rev. B* **107**, 035133 (2023).
- [23] F. D. M. Haldane, S. Raghu, “Possible realization of directional optical waveguides in photonic crystals with broken time-reversal symmetry”, *Phys. Rev. Lett.* **100**, 013904 (2008).
- [24] Z. Wang, Y. Chong, J. D. Joannopoulos, M. Soljačić, “Observation of unidirectional backscattering-immune topological electromagnetic states”, *Nature (London)* **461**, 772 (2009).
- [25] W. Zhao, S. Zhao, H. Li, S. Wang, S. Wang, M. I. B. Utama, S. Kahn, Y. Jiang, X. Xiao, S. Yoo *et al.*, “Efficient Fizeau drag from Dirac electrons in monolayer graphene”, *Nature (London)* **594**, 517 (2021).
- [26] T. A. Morgado, M. G. Silveirinha, “Drift-induced unidirectional graphene plasmons”, *ACS Photonics* **5**, 4253 (2018).
- [27] T. A. Morgado, M. G. Silveirinha, “Nonlocal effects and enhanced nonreciprocity in current-driven graphene systems”, *Phys. Rev. B* **102**, 075102 (2020).
- [28] CST Microwave Studio – Computer Simulation Technology: <http://www.cst.com>, Oct. 2014.

## Supplemental Information:

### *Gain-Momentum Locking in a Chiral-Gain Medium*

João C. Serra<sup>1,‡</sup>, Nader Engheta<sup>2</sup>, Mário G. Silveirinha<sup>1,§</sup>

<sup>(1)</sup> *University of Lisbon–Instituto Superior Técnico and Instituto de Telecomunicações, Avenida Rovisco Pais, 1, 1049-001 Lisboa, Portugal*

<sup>(2)</sup> *University of Pennsylvania, Department of Electrical and Systems Engineering, Philadelphia, PA 19104, U.S.A.*

The supplemental information provides additional details on A) bulk stability of the non-dispersive material, B) dispersion of the edge states at an interface between a chiral-gain medium and an isotropic material, C) bulk stability of the dispersive material.

#### ***A. Bulk stability of the non-dispersive material***

In this supplementary note, we analyze the bulk response stability of the chiral-gain medium. For simplicity, we restrict our attention to the case of propagation in the  $xoz$  plane. The bulk modes are plane waves of the type  $\mathbf{E}(\mathbf{r}, t) = \mathbf{E}_0 e^{i\mathbf{k}\cdot\mathbf{r}} e^{-i\omega t}$ . The corresponding dispersion equation is:

$$\mathbf{k} \times (\mathbf{k} \times \mathbf{E}_0) + \frac{\omega^2}{c^2} \bar{\boldsymbol{\epsilon}} \cdot \mathbf{E}_0 = \mathbf{0}. \quad (\text{S1})$$

For a relative permittivity tensor as in the main text

---

‡ E-mail: [joao.serra@lx.it.pt](mailto:joao.serra@lx.it.pt)

§ To whom correspondence should be addressed: [mario.silveirinha@tecnico.ulisboa.pt](mailto:mario.silveirinha@tecnico.ulisboa.pt)

$$\bar{\boldsymbol{\varepsilon}} = \begin{pmatrix} \varepsilon_{xx} & 0 & \varepsilon_{xz} \\ 0 & \varepsilon_{yy} & 0 \\ 0 & 0 & \varepsilon_{zz} \end{pmatrix}, \quad (\text{S2})$$

and for propagation in the  $xoz$  plane, we find that the chiral-gain material supports two independent bulk modes:

$$\mathbf{E}_1 \sim e^{ik_x x} e^{ik_z z} e^{-i\omega t} \hat{\mathbf{y}}, \quad \omega = c \sqrt{\frac{k_x^2 + k_z^2}{\varepsilon_{yy}}} \quad (\text{S3a})$$

$$\mathbf{E}_2 \sim e^{ik_x x} e^{ik_z z} e^{-i\omega t} \left[ \left( k_x^2 - \varepsilon_{zz} \frac{\omega^2}{c^2} \right) \hat{\mathbf{x}} + k_x k_z \hat{\mathbf{z}} \right], \quad \omega = c \sqrt{\frac{k_x^2 \varepsilon_{xx} + k_z^2 \varepsilon_{zz} + k_x k_z \varepsilon_{xz}}{\varepsilon_{xx} \varepsilon_{zz}}}. \quad (\text{S3b})$$

It is straightforward to check that for  $\mathbf{k} = k_x \hat{\mathbf{x}} + k_z \hat{\mathbf{z}}$  real-valued, the eigenfrequencies are

also real-valued provided  $\varepsilon_{xx} \varepsilon_{zz} - \left( \frac{\varepsilon_{xz}}{2} \right)^2 > 0$ , or equivalently  $|\varepsilon_{xz}| < 2\sqrt{\varepsilon_{xx} \varepsilon_{zz}}$ . It is relevant

to note that for a stable system the eigenpolarizations of the material are linearly polarized.

Hence, all the components of  $\mathbf{E}_1$  ( $\mathbf{E}_2$ ) are in-phase.

### ***B. Dispersion of the edge states at an interface between a chiral-gain medium and an isotropic material***

Next, we deduce the exact edge dispersion for surface plasmons propagating at the flat interface (Fig. 1b of the main text) between a chiral-gain material and an isotropic material with relative permittivity  $\varepsilon_m(\omega)$ .

For the horizontal interface  $x = 0$  (with the chiral-gain material in the half-space  $x < 0$ ), we look for transverse magnetic (TM) waves ( $\mathbf{H} = H\hat{\mathbf{y}}$ ) with the following structure:

$$H(x, z, t) = H_0 e^{-i\omega t} e^{iqz} \times \begin{cases} e^{+\gamma_c x}, & x < 0 \\ e^{-\gamma_m x}, & x > 0 \end{cases}. \quad (\text{S4})$$

Here,  $\gamma_m = \sqrt{q^2 - \frac{\omega^2}{c^2} \epsilon_m(\omega)}$  is the attenuation constant (along  $x$ ) in the isotropic region,

whereas  $\gamma_c$  is the attenuation constant in the chiral-gain medium region. From Eq. (S3b),

it is readily found that:

$$\gamma_c = \sqrt{q^2 \left( \frac{\epsilon_{zz}}{\epsilon_{xx}} - \frac{\epsilon_{xz}^2}{4\epsilon_{xx}^2} \right) - \frac{\omega^2}{c^2} \epsilon_{zz}} - iq \frac{\epsilon_{xz}}{2\epsilon_{xx}}. \quad (\text{S5})$$

The electric field can be obtained from Ampère's law as  $\mathbf{E} = \frac{1}{-i\omega\epsilon_0} \epsilon^{-1} \cdot (\nabla H \times \hat{\mathbf{y}})$ .

Therefore, the continuity of the tangential electric field ( $E_z$ ) at the interface  $x = 0$  implies

that  $\frac{1}{\epsilon_{zz}} \partial_x H$  is also continuous. This leads to the exact edge dispersion equation:

$$\frac{\gamma_c}{\epsilon_{zz}} + \frac{\gamma_m}{\epsilon_m(\omega)} = 0. \quad (\text{S6})$$

Similarly, for the vertical interface  $z = 0$  (with the chiral-gain material in the half-space  $z > 0$ ), we look for TM waves characterized by the magnetic field distribution

$$H(x, z, t) = H_0 e^{-i\omega t} e^{iqx} \times \begin{cases} e^{+\gamma_m z}, & z < 0 \\ e^{-\tilde{\gamma}_c z}, & z > 0 \end{cases} \quad (\text{S7})$$

with the attenuation constant  $\tilde{\gamma}_c = \sqrt{q^2 \left( \frac{\epsilon_{xx}}{\epsilon_{zz}} - \frac{\epsilon_{xz}^2}{4\epsilon_{zz}^2} \right) - \frac{\omega^2}{c^2} \epsilon_{xx}} + iq \frac{\epsilon_{xz}}{2\epsilon_{zz}}$ . Imposing the

continuity of the tangential electric field ( $E_x$ ), we obtain the dispersion equation:

$$\frac{\tilde{\gamma}_c}{\epsilon_{xx}} + \frac{\gamma_m}{\epsilon_m(\omega)} - iq \frac{\epsilon_{xz}}{\epsilon_{xx} \epsilon_{zz}} = 0. \quad (\text{S8})$$

In the quasi-static limit ( $|q| \gg |\omega|/c$ ), one can use  $\gamma_c \approx \gamma_{c0}$ ,  $\tilde{\gamma}_c \approx \tilde{\gamma}_{c0}$  and  $\gamma_m \approx \gamma_{m0}$  where  $\gamma_{c0}$ ,  $\tilde{\gamma}_{c0}$ ,  $\gamma_{m0}$  are defined as in the main text. Substituting these approximations into Eq. (S6) [Eq. (S8)] and solving with respect to  $\omega$ , it can be shown that the equation yields the same result as Eq. (4). Interestingly, this coincidence occurs even though the exact and quasi-static dispersion equations have quite different structures.

### C. Bulk stability of the dispersive material

In this supplementary note, we analyze the stability of a dispersive chiral-gain medium with a Drude-type diagonal response:

$$\varepsilon_{xx} = \varepsilon_{zz} = \varepsilon_c(\omega) = \varepsilon_\infty - \frac{\omega_p^2}{\omega(\omega + i\gamma)}. \quad (\text{S9})$$

Similar to Section A, we restrict our attention to propagation in the  $xoz$  plane and to transverse magnetic (TM) waves. From Eq. (S3b), TM-polarized bulk plane waves are governed by the dispersion relation

$$\omega^2 \varepsilon_c^2(\omega) = c^2 k^2 \left( \varepsilon_c(\omega) + \frac{\sin(2\phi)}{2} \varepsilon_{xz} \right), \quad (\text{S10})$$

where we write the wave vector as  $\mathbf{k} = k(\cos\phi\hat{\mathbf{x}} + \sin\phi\hat{\mathbf{z}})$ . It is convenient to rewrite this equation as

$$\frac{\tilde{\omega}^2 - \tilde{\gamma}^2}{(\tilde{\omega}^2 + \tilde{\gamma}^2)^2} + \frac{\tilde{k}^2 - 2\tilde{\omega}^2}{\tilde{\omega}^2 + \tilde{\gamma}^2} + \tilde{\omega}^2 - A_{\mathbf{k}} = i \frac{\tilde{\gamma}}{\tilde{\omega}^2 + \tilde{\gamma}^2} \left[ \frac{2\tilde{\omega}}{\tilde{\omega}^2 + \tilde{\gamma}^2} + \frac{\tilde{k}^2 - 2\tilde{\omega}^2}{\tilde{\omega}} \right], \quad (\text{S11})$$

where we have defined the dimensionless parameters  $\tilde{\omega} = \frac{\sqrt{\varepsilon_\infty} \omega}{\omega_p}$ ,  $\tilde{k} = \frac{ck}{\omega_p}$ ,  $\tilde{\gamma} = \frac{\sqrt{\varepsilon_\infty} \gamma}{\omega_p}$ ,

$$\Sigma = \frac{\varepsilon_{xz}}{\varepsilon_\infty} \text{ and } A_{\mathbf{k}} = \tilde{k}^2 \left( 1 + \frac{\sin(2\phi)}{2} \Sigma \right).$$

If  $\gamma = 0$ , there are two independent branches governed by

$$\tilde{\omega}^2 = 1 + \frac{A_{\mathbf{k}}}{2} \pm \sqrt{\left( 1 + \frac{A_{\mathbf{k}}}{2} \right)^2 - (1 + \tilde{k}^2)}. \text{ In this case, when } \varepsilon_{xz} \neq 0 \text{ the radicand can always be}$$

negative for sufficiently small  $\tilde{k} \neq 0$ , and consequently there are always solutions in the upper-half frequency plane for some real-valued wave vector  $\mathbf{k}$ , implying that the bulk response is unstable. Hence, the collision frequency  $\gamma$  is essential to stabilize the bulk response.

On the other hand, without the chiral-gain ( $\Sigma = 0$ ), it is evident that when  $\tilde{\gamma} > 0$  the spectrum must lie in the lower-half frequency plane for  $\tilde{k}$  real-valued because of the absorption intrinsic to the Drude dispersion model. For a fixed  $\tilde{\gamma}$ , the response may become unstable, i.e., some roots of (S11) may move towards the upper-half-frequency plane as  $|\Sigma|$  increases. Clearly, at the threshold gain that marks the transition from stability to instability the spectrum will intersect the real-frequency axis at exactly one point along the directions  $\phi \in \left\{ -\frac{\pi}{4}, \frac{3\pi}{4} \right\}$  for  $\Sigma > 0$  and  $\phi \in \left\{ -\frac{3\pi}{4}, \frac{\pi}{4} \right\}$  for  $\Sigma < 0$ . Equivalently, if the band structure does not intersect the real frequency axis inside some compact set of the  $(\Sigma, \tilde{\gamma})$  parameters space containing  $(\Sigma = 0, \tilde{\gamma} = 0)$ , then the bulk response is always stable for that set of parameters.

Let us suppose that there is in fact a real-valued frequency  $\tilde{\omega}$  that satisfies Eq. (S11)

for  $(\tilde{k}, \phi)$  real-valued with  $\tilde{\gamma} > 0$ . Then, both sides of Eq. (S11) must vanish:

$$\begin{cases} \frac{\tilde{\omega}^2 - \tilde{\gamma}^2}{(\tilde{\omega}^2 + \tilde{\gamma}^2)^2} + \frac{\tilde{k}^2 - 2\tilde{\omega}^2}{\tilde{\omega}^2 + \tilde{\gamma}^2} + \tilde{\omega}^2 - A_{\mathbf{k}} = 0 \\ \frac{\tilde{\gamma}}{\tilde{\omega}^2 + \tilde{\gamma}^2} \left[ \frac{2\tilde{\omega}}{\tilde{\omega}^2 + \tilde{\gamma}^2} + \frac{\tilde{k}^2 - 2\tilde{\omega}^2}{\tilde{\omega}} \right] = 0 \end{cases} \Leftrightarrow \begin{cases} 1 - (\tilde{\omega}^2 - A_{\mathbf{k}})(\tilde{\omega}^2 + \tilde{\gamma}^2) = 0 \\ 2\tilde{\omega}^2 + (\tilde{k}^2 - 2\tilde{\omega}^2)(\tilde{\omega}^2 + \tilde{\gamma}^2) = 0 \end{cases}. \quad (\text{S12})$$

By substituting the solution of the first equation, i.e.,

$$\tilde{\omega}^2 = \frac{A_{\mathbf{k}} - \tilde{\gamma}^2}{2} \pm \sqrt{\frac{(A_{\mathbf{k}} + \tilde{\gamma}^2)^2}{4} + 1}, \quad (\text{S13})$$

into the second equation, we obtain

$$a_{\phi} \tilde{k}^4 + 2b_{\phi} \tilde{k}^2 + 4\tilde{\gamma}^2 = 0 \Leftrightarrow \tilde{k}^2 = \frac{-b_{\phi} \pm \sqrt{b_{\phi}^2 - 4\tilde{\gamma}^2 a_{\phi}}}{a_{\phi}}, \quad (\text{S14})$$

with

$$a_{\phi} = (1 + \Sigma \sin(2\phi)) \left[ 1 + (2 + \Sigma \sin(2\phi)) \tilde{\gamma}^2 \right], \quad (\text{S15})$$

$$b_{\phi} = (1 + \Sigma \sin(2\phi)) \tilde{\gamma}^4 - \tilde{\gamma}^2 + \Sigma \sin(2\phi). \quad (\text{S16})$$

Importantly, Eq. (S14) yields real-valued  $\tilde{k}$  solutions, i.e., the band structure intersects the real-frequency axis, if and only if  $b_{\phi}^2 - 4a_{\phi}\tilde{\gamma}^2 \geq 0$  and  $a_{\phi} < 0 \vee b_{\phi} \leq 0$  for some  $\phi$ .

Therefore, by enforcing  $b_{\phi}^2 - 4a_{\phi}\tilde{\gamma}^2 < 0$  or  $a_{\phi}, b_{\phi} > 0$  for all  $\phi$ , we obtain the bulk stability condition:

$$|\Sigma| < 1 - \frac{1}{(1 + \tilde{\gamma})^2}. \quad (\text{S17})$$

The critical cases correspond to  $\sin(2\phi) = \pm 1$ .



The shaded yellow region in Fig. S1 represents the chiral-gain range for which the bulk response is stable for a certain dissipation level  $\tilde{\gamma}$ . When  $|\Sigma| \geq 1$ , the bulk response is always unstable.

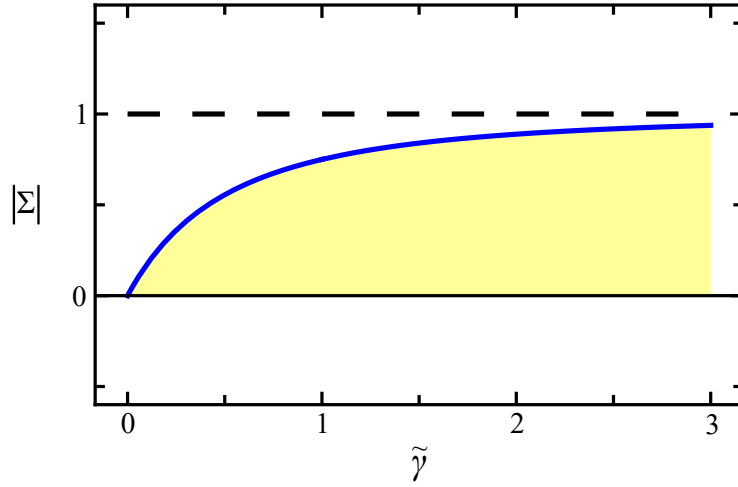


**Fig. S1** The region shaded in yellow represents the range of the normalized gain ( $\Sigma = \varepsilon_{xz} / \varepsilon_{xx}$ ) that provides a stable bulk response for the dispersive chiral-gain medium. The normalized dissipation level is

$$\tilde{\gamma} = \sqrt{\varepsilon_{xx}} \gamma / \omega_p.$$